Hindawi Publishing Corporation
International Journal of Photoenergy
Volume 2012, Article ID 794207, 7 pages
doi:10.1155/2012/794207

Research Article

Nitrogen-Doped TiO_2 Nanotube Arrays with Enhanced Photoelectrochemical Property

Shipu Li, Shiwei Lin, Jianjun Liao, Nengqian Pan, Danhong Li, and Jianbao Li

Key Laboratory of Ministry of Education for Application Technology of Chemical Materials in Hainan Superior Resources, School of Materials and Chemical Engineering, Hainan University, Haikou 570228, China

Correspondence should be addressed to Shiwei Lin, linsw@hainu.edu.cn

Received 22 January 2012; Revised 22 February 2012; Accepted 27 February 2012

Academic Editor: Xuxu Wang

N-doped TiO_2 nanotube arrays were prepared by electrochemical anodization in glycerol electrolyte, followed by electrochemical deposition in NH_4Cl solution. An orthogonal experiment was used to optimize the doping conditions. Electrolyte concentration, reaction voltage, and reaction time were the main factors to influence the N-doping effect which was the determinant of the visible range photoresponse. The optimal N-doping conditions were determined as follows: reaction voltage is 3 V, reaction time is 2 h, and electrolyte concentration is 0.5 M. The maximal photocurrent enhanced ratio was 30% under white-light irradiation. About 58% improvement of photocatalytic efficiency was achieved in the Rhodamine B degradation experiment by N doping. The kinetic constant of the N-doped TNT arrays sample was almost twice higher than that of the undoped sample. Further analysis by X-ray photoelectron spectroscopy supported that electrochemical deposition is a simple and efficient method for N doping into TiO_2 nanotube arrays.

1. Introduction

Since the discovery of water photolysis on TiO_2 electrode by Fujishima and Honda in 1972 [1], TiO_2 has been extensively studied. It is one of the most promising oxide semiconductors for photoelectrochemical applications, particularly due to its low cost, nontoxicity, and stability against photocorrosion. In contrast to nanoparticle, highly ordered TiO_2 nanotube (TNT) arrays not only have high surface-to-volume ratios and adsorptive capacity, but also have good photocatalytic properties and high photoelectrical conversion efficiency. Also, the nanotubes produced by anodization can permit a careful control over their nanotube diameter, layer thickness, and wall thickness, obtaining structures vertically oriented from the surface. So the TNT arrays have widespread application prospect in dye sensitization solar cells, sensors, hydrogen generation by water photoelectrolysis, photocatalytic degradation of pollutants, and biomedicines [2–11].

However, due to the comparably large bandgap (anatase, Eg ~ 3.2 eV), TiO_2 can only respond to UV light irradiation ($\lambda < 380$ nm) which possesses about 4% of the solar spectrum. This greatly limits its application prospects. To overcome this problem, two different strategies have been typically taken: element doping and surface modification. Asahi et al. reported that improved photocatalytic activity of TiO_2 under visible light irradiation can be achieved by nitrogen doping [12]. Since then, many preparation methods, such as ion implantation, hydrothermal, chemical vapor deposition, chemical liquid deposition, and anodic oxidation of Ti/N alloy [13–19], have been reported to dope nitrogen into TiO_2 using different N-doped precursors to enhance the photoelectrochemical properties of TiO_2. However their doping effects are contradictory, and the underlying mechanisms are also lack of a consensus.

In our previous work, we reported the successful controllable growth of highly ordered TiO_2 nanotube arrays by adjusting the anodization voltage and duration [20]. In this paper, we investigate a simple and efficient nitrogen-doping approach, that is, electrochemical deposition. Despite the vast reports on TNT arrays, there is little research on the influence of doping parameters on electrochemical nitrogen-doping process. Thus, we take an orthogonal experiment to optimize the doping conditions in order to obtain an excellent visible range photoresponse. Then, the N-doping

Table 1: Factors and levels for orthogonal experiments.

Factors	Levels		
	1	2	3
(A) Electrolyte concentration (M)	0.5	1	1.5
(B) Reaction voltage (V)	1	2	3
(C) Reaction time (h)	1	2	3

effect on the photocatalytic activity is further characterized by the degradation of Rhodamine B under simulated sunlight irradiation.

2. Experimental

2.1. Preparation of TiO_2 Nanotube Arrays. The TiO_2 nanotube arrays were prepared by electrochemical anodization of titanium foils (0.5 mm thickness, 99.4% purity). Firstly, the titanium foils were cut into small pieces (1.5 × 5 cm) and polished by chemical polishing fluid ($HF : HNO_3 = 1 : 4$, in volumetric ratio). Then all of the foils were degreased by sonication in acetone, methanol, deionized (DI) water, respectively, and finally dried in air. The anodization was performed in a two-electrode configuration with titanium foil as the working electrode and stainless steel foil as the counterelectrode. The distance between two electrodes was kept at 2.5 cm. The samples were anodized at 30 V and in solutions containing 0.27 M NH_4F consisting of mixtures of DI water and glycerol (1, 2, 3-propanetriol) prepared in volumetric ratio of 50 : 50% for 3 h. After the electrochemical treatment the samples were rinsed with DI water and dried in air.

2.2. N-Doping Approach. The as-prepared TiO_2 nanotube arrays (on Ti sheet) were used as the cathode and platinum as the anode. The electrolyte was NH_4Cl solution. The distance between two electrodes was kept at 2.5 cm. The electrochemical deposition process was performed at different potentials for various reaction durations. Then, the sample was taken out and rinsed with DI water. Thermal annealing was performed in ambient air at 450°C for 3 h. An orthogonal experiment was used to investigate the optimal doping condition. As seen from Table 1, the doping experiments were carried out with 3 factors and 3 levels, namely, electrolyte concentration (0.5, 1, and 1.5 M), reaction voltage (1, 2, and 3 V), and reaction time (1, 2, and 3 h), respectively. The range of each factor level was determined based on the results of preliminary experiments. The photocurrent enhancement ratio of the doped samples under visible light irradiation relative to the undoped sample was used as the dependent variable to determine the optimal doping condition.

2.3. Morphology and Structure Characterization of TNT Arrays. The morphologies of the as-prepared samples were observed using a field-emission scanning electron microscope (FESEM, Hitachi, S-4800) and their crystalline phase was identified using an X-ray diffraction (XRD, Bruker AXS, D8 Advance) technique. The surface chemical composition of the samples was analyzed by X-ray photoelectron spectroscopy (XPS, PHI-5300) with Al Kα radiation source. The absorption properties of the samples were recorded using a diffuse reflectance UV-vis spectrometer (Persee, TU-1901) with the wavelength range between 250 and 750 nm.

2.4. Photoelectrochemical and Photocatalytic Properties. Photocurrent densities were measured using an electrochemical workstation (Zahner, Zennium) in a standard three-electrode configuration with a platinum foil as the counter-electrode, a saturated calomel electrode (SCE) as the reference electrode, and the TNT arrays sample as the working electrode. 1 M KOH was used as the electrolyte. A self-contained white light source with intensity of 12 mW/cm^2 was utilized as an excitation source (dominant wavelength: 553 nm, half intensity line width: Δ119 nm).

To compare the photocatalytic activity of the undoped and N-doped TiO_2 photocatalysts, photocatalytic degradation experiments were performed. Rhodamine B (Rh B) was chosen as a target compound. The initial concentration of the dye was 5 mg/L and the pH value of the Rh B solution was 7. A 500 W xenon lamp was used to produce the simulated sunlight. Before the photocatalytic degradation, the photocatalyst (3.0 cm × 1.5 cm) was soaked in 10 mL Rh B solution for 30 min to establish the adsorption/desorption equilibrium. The concentration of Rh B was then determined at 554 nm every 30 min by the UV-vis spectrophotometer (Persee, TU-1901). The blank test was also carried out by irradiating Rh B solution without TiO_2 photocatalyst for checking the self-photolysis of Rh B.

3. Results and Discussion

3.1. SEM Analysis. Figure 1 shows FESEM images of the undoped and N-doped TNT arrays samples. Since the morphologies of all the N-doped TNT arrays samples are similar, we chose a representative sample, with the reaction voltage of 3 V, reaction time of 3 h, and electrolyte concentration of 0.5 M, to make the results more clear and simple. The obtained nanotube arrays show highly ordered and vertically oriented morphology with inner diameter approximately 140 nm, and the nanotube length is about 2.1 μm. It can be clearly seen that the nanotube arrays keep its structural integrity after the nitrogen doping electrochemical process.

3.2. XRD Analysis. The XRD patterns of the as-prepared TNT arrays sample, the annealed undoped sample, and the annealed N-doped TNT arrays sample are shown in Figure 2. The as-prepared TNT arrays film exhibits an amorphous structure with the existence of only typical diffraction peaks of metallic titanium. Hence, the annealing process is necessary to transfer the amorphous TiO_2 film into a well-crystallized phase. Upon thermal annealing the samples at 450°C for 3 h, two anatase diffraction peaks at 25.5° (101), and 48.1° (200) can be clearly observed, indicating that the TNT arrays samples had been crystallized. In addition, the undoped sample has more obvious rutile peaks than the N-doped sample. This suggests that the phase transition from

Table 2: Results of the orthogonal experiment.

No.	(*A*) Electrolyte concentration (*M*)	(*B*) Reaction voltage (*V*)	(*C*) Reaction time (*h*)	Photocurrent enhancement ratio (%)
1	0.5	1	1	9.0
2	0.5	2	2	11.5
3	0.5	3	3	30.0
4	1	1	2	16.0
5	1	2	3	13.2
6	1	3	1	18.5
7	1.5	1	3	9.0
8	1.5	2	1	6.2
9	1.5	3	2	25.9
K_1	16.8	11.3	11.2	
K_2	15.9	10.3	17.8	
K_3	13.7	23.0	17.4	
R	3.1	12.7	6.6	

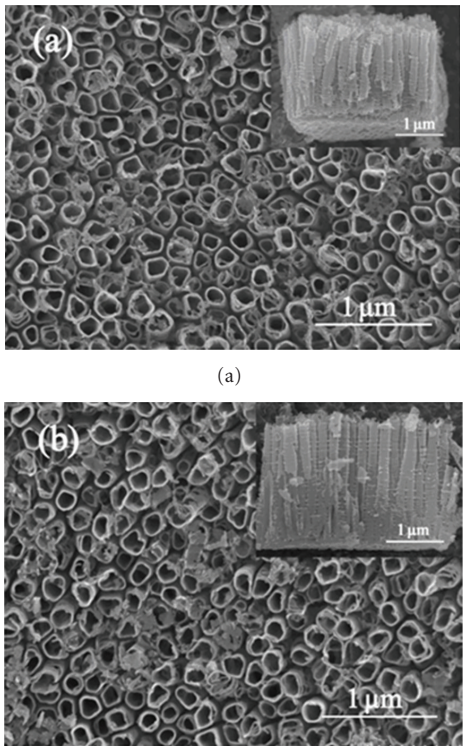

Figure 1: FESEM top images of the (a) undoped and (b) N-doped TNT arrays samples. The doping conditions are that reaction voltage is 3 V, reaction time 3 h, and electrolyte concentration 0.5 M. The insets show the corresponding cross-sectional images.

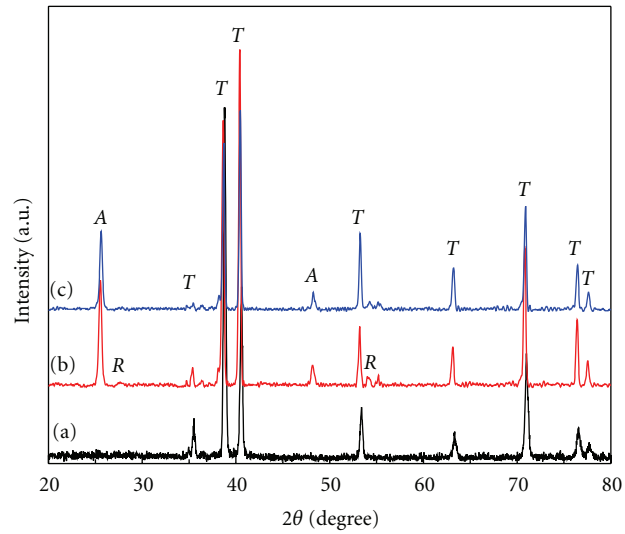

Figure 2: XRD patterns of (a) the as-prepared TNT arrays sample, (b) the undoped TNT arrays sample annealed at 450°C for 3 h, and (c) N-doped TNT arrays sample after annealing at 450°C for 3 h. The doping conditions are that reaction voltage is 3 V, reaction time 3 h, and electrolyte concentration 0.5 M. *A*, *R*, and *T* represent anatase, rutile, and titanium, respectively.

anatase to rutile during annealing might be inhibited by the incorporation of N dopant in the TiO_2 lattice [17].

3.3. UV-Vis Absorption Spectroscopic Analysis. Figure 3 compares the UV-visible diffuse reflectance spectra of the undoped and the N-doped TNT arrays. TiO_2 absorption threshold localizes between 350 and 380 nm, and a shift toward the visible light region is observed for the N-doped sample. The broad absorption peaks between 400 and 600 nm are attributed to the subbandgap states of the TNT arrays due to the special nanotube structure [21], which makes it difficult to accurately determine the UV-vis absorption for the pure TNT arrays. So, further photoeletrochemical characterization and measurements should be performed to clarify the N-doping effects.

3.4. Photoelectrochemical Property and Orthogonal Test Results. The photocurrent response measurements were performed under visible light pulsed irradiation to investigate the photoinduced charge separation efficiency of the undoped and N-doped samples. The results are shown in

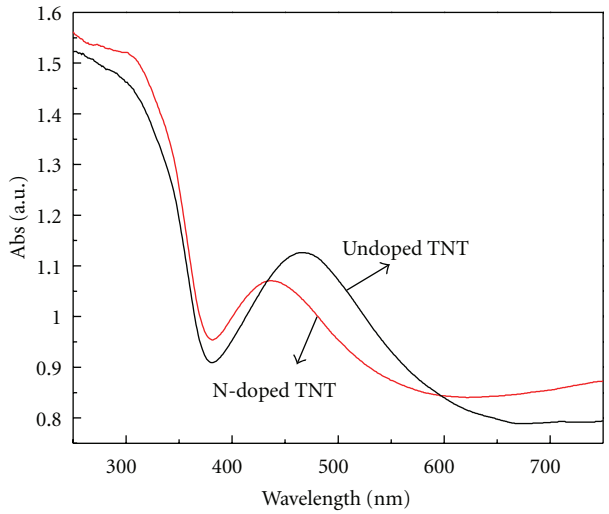

Figure 3: UV-vis absorption spectra of the undoped and N-doped TNT arrays. The doping conditions are that reaction voltage is 3 V, reaction time 3 h and electrolyte concentration 0.5 M.

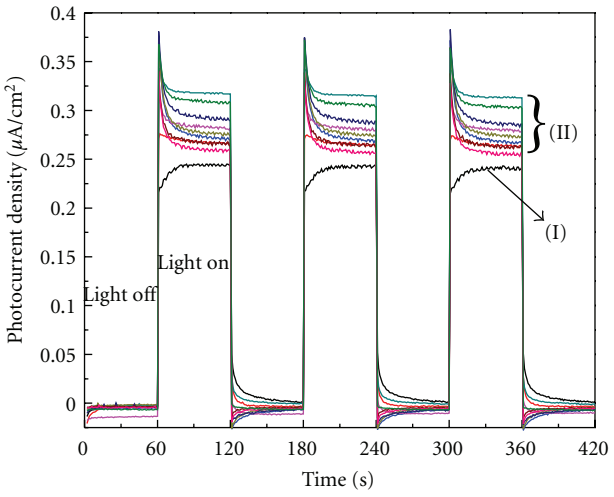

Figure 4: Photocurrent response of (I) undoped TNT and (II) N-doped TNT arrays samples.

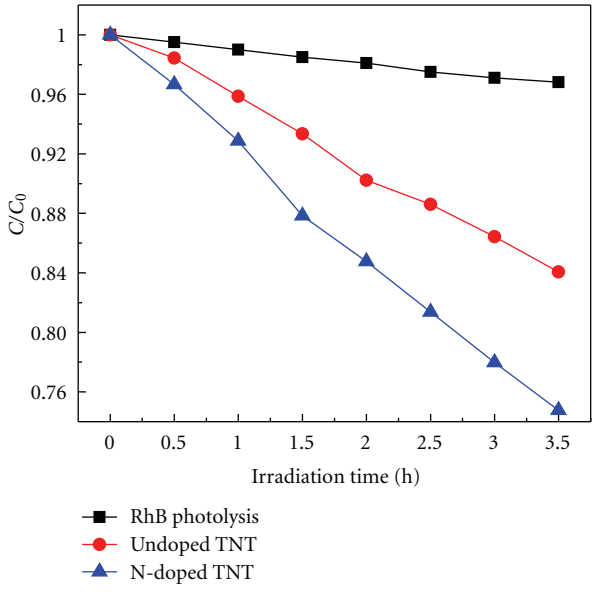

(a)

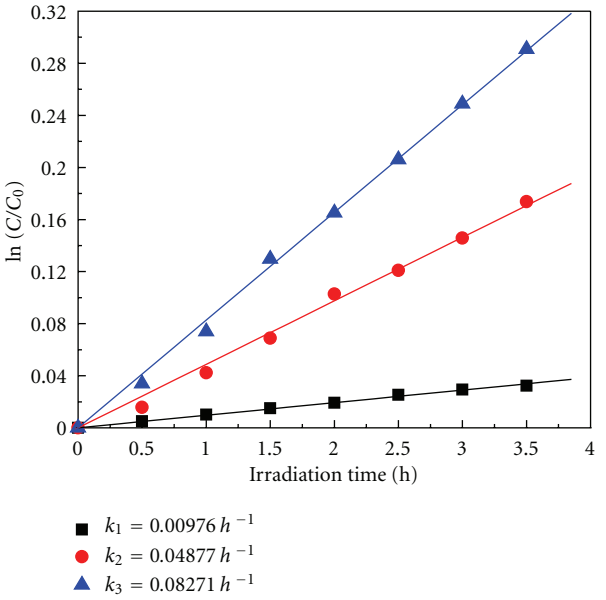

(b)

Figure 5: Comparison of (a) degradation rates and (b) kinetic curves by the Rh B degradation using the undoped TNT and N-doped TNT arrays samples. The doping conditions are that reaction voltage is 3 V, reaction time 3 h and electrolyte concentration 0.5 M.

Figure 4. The working electrode potential was set at 0 V to keep the same working condition. All the N-doped samples, treated under different doping conditions, possess higher photocurrents than the undoped ones. We can see that the highest photocurrent of the N-doped TNT arrays (0.316 μA/cm^2) is much higher than the undoped sample, which is 0.243 μA/cm^2. However, as well known pure TiO_2 can only respond to UV light, as the excitation source (dominant wavelength: 553 nm, half intensity line width: Δ119 nm) contains a little UV light, the undoped sample got a small photocurrent. Higher photocurrent means more photoinduced carriers can transfer from N-doped TNT to the counterelectrode via external circuit. The photocatalytic activity of titania greatly depends on the electron-hole transfer ability [22]. Therefore, it can be expected that the N-doped samples should have better photocatalytic activity as compared to the undoped sample.

The photoelectrochemical property of N-doped TNT arrays was also found to be strongly dependent on the doping conditions. Electrolyte concentration, reaction voltage, and reaction time are the three most important factors that influence the N-doping effect during the electrochemical deposition process. The independent variables with three variation levels, X1 (electrolyte concentration: 0.5, 1, and 1.5 M),

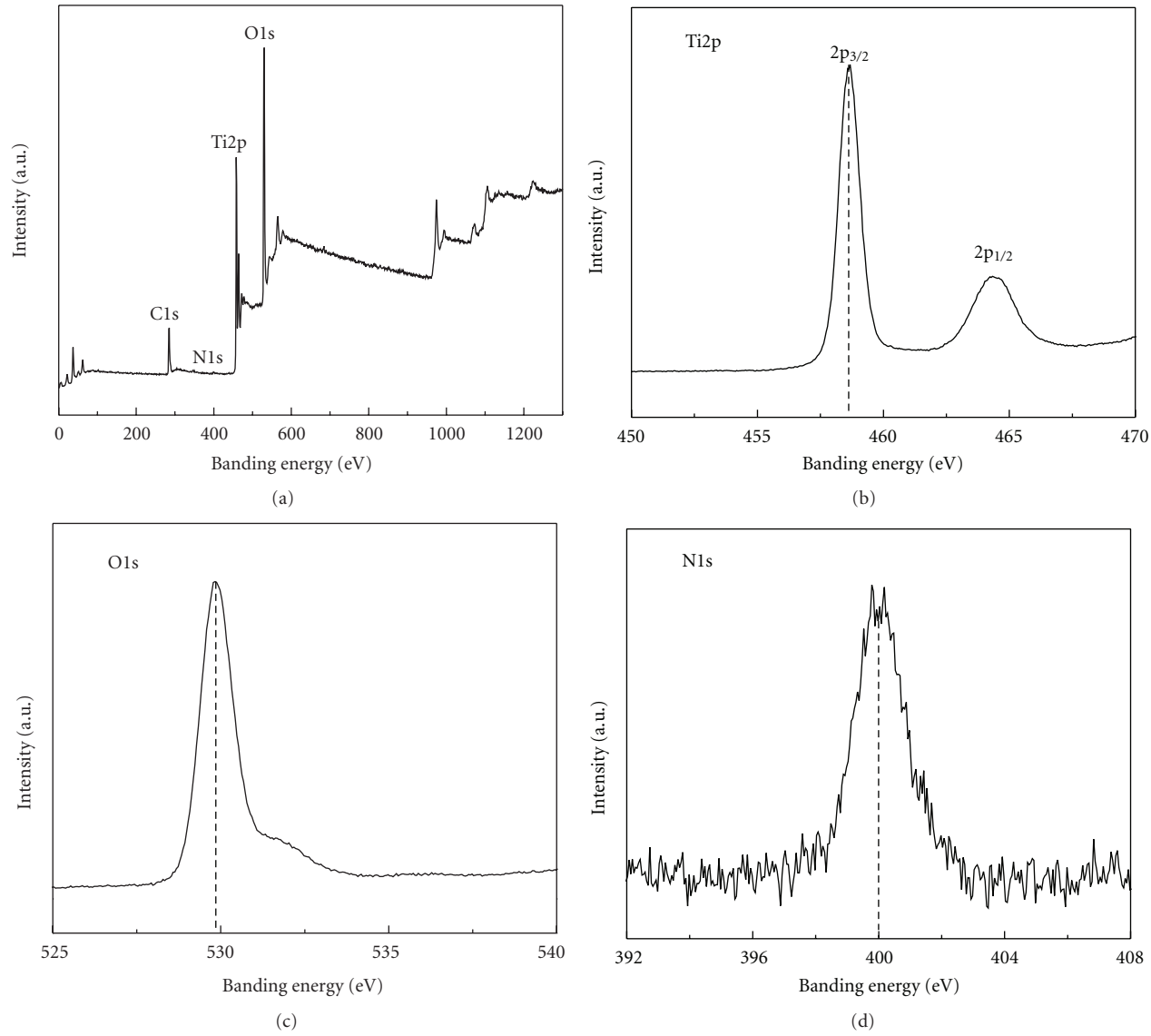

Figure 6: XPS spectra of the N-doped TNT arrays sample. (a) A survey spectrum, (b) a spectrum of Ti 2p, (c) a spectrum of O 1s, and (d) a spectrum of N 1s. The doping conditions are that reaction voltage is 3 V, reaction time 3 h and electrolyte concentration 0.5 M.

X2 (reaction voltage: 1, 2, and 3 V), and X3 (reaction time: 1, 2, and 3 h) are listed in Table 1. To compare the N-doping effect more clearly, the photocurrent enhancement ratio of the N-doped samples relative to the undoped one was chosen as the dependent variable. The analysis results of the orthogonal experiment are presented in Table 2. Although the maximum photocurrent enhancement ratio was 30%, we cannot choose the corresponding extraction condition as the best condition. In view of orthogonal analysis, we calculated the values of K and R. K_i ($i = 1, 2, 3$) is the average of the sum of photocurrent enhancement ratio for certain factor at level i, and R refers to the result of extreme analysis. According to the R value, the factors which influence the photocurrent enhancement ratio are listed in a decreasing order: $B > C > A$. Based on the K value, we can see that the photocurrent enhancement ratio decreases with increasing electrolyte concentration. When the reaction voltage is 3 V, the enhancement ratio has the maximum value. And the photocurrent enhancement ratio increases with the increasing reaction time and reaches the peak value at 2 h and then drops from 2 to 3 h. So, with respect to the photocurrent enhancement ratio, the optimal condition is obtained when electrolyte concentration, reaction voltage, and reaction time are $B_3C_2A_1$, that are 3 V, 2 h and 0.5 M, respectively. However, according to the K value, the difference between 2 and 3 h is very little, and the reaction time is relatively secondary factor, so we chose the sample, with the reaction voltage of 3 V, reaction time of 3 h, and electrolyte concentration of 0.5 M, to perform further characterization and measurements.

3.5. Photocatalytic Activity. In order to further study the N-doping effect, the photocatalytic activity of the undoped

and N-doped TNT arrays samples was studied using the degradation of Rh B solution, and the results are shown in Figure 5. Direct photodegradation ability was also studied, and only less than 4% of Rh B was decomposed. After 3.5 h visible light irradiation, the Rh B degradation efficiencies were determined as 16% and 25.7%, for the undoped and N-doped TNT arrays samples, respectively. The doping conditions are reaction voltage 3 V, reaction time 3 h, and electrolyte concentration 0.5 M. About 58% improvement of photocatalytic efficiency is achieved by N doping.

The apparent first-order kinetic equation is $\ln(C_0/C) = kt$, where k is the reaction rate constant, t is the irradiation time, and C_0 and C are the initial and reaction concentrations of Rh B aqueous solutions, respectively. The variations in $\ln(C_0/C)$ as a function of irradiation time are given in Figure 5(b). It can be seen that the Rh B photodegradation clearly obeyed the first-order reaction kinetics. And the apparent rate constant k of the TiO_2 nanotube photocatalyst is significantly higher than that of Rh B photolysis, indicating that TiO_2 plays an important role in the photocatalytic process. The k value of the undoped TNT arrays sample is $0.04877\,h^{-1}$, while the reaction rate constant of the N-doped sample is $0.08271\,h^{-1}$. The kinetic constant of the N-doped sample is almost twice higher than that of the undoped sample, suggesting that its photocatalytic activity driven by visible light can be enhanced by the electrochemical N-doping deposition method.

3.6. XPS Analysis. The elemental composition of the N-doped TNT arrays sample was determined by XPS. Figure 6(a) shows that the surface of the TNT arrays is composed of Ti, O, C, and N elements. The residual carbon from electrolyte and adventitious element carbon may cause the presence of C element [23]. From Figure 6(b), it can be seen that Ti $2p_{3/2}$ core level appears at 458.6 eV. The binding energy in the N-doped TNT arrays sample is lower than the undoped sample (458.7 eV, not shown here), suggesting that TiO_2 lattice is modified due to N-substitution [24, 25]. Oxygen 1s core level peak appears around 530 eV, as shown in Figure 6(c). A feature extending to higher binding energy at about 532 eV is clearly visible, suggesting the presence of another type of oxygen due to the more covalent nature of the N-doped TNT arrays sample. This might be due to the presence of oxygen and nitrogen from the same lattice units in TiO_2 [25]. Figure 6(d) shows the XPS spectrum of N 1s core level of the N-doped TNT arrays. Only a single peak at about 400 eV can be found, which was due to the N^- anion incorporated in the TiO_2 as N-Ti-O structural feature [24–27]. This is in good agreement with the XPS findings by Chen et al. [24] and Sathish et al. [25].

4. Conclusions

Nitrogen-doped TiO_2 nanotube arrays were prepared by a simple electrochemical deposition method. By comparing the FESEM images of undoped and N-doped TNT, the TiO_2 nanotube arrays kept their structural integrity with inner diameter approximately 140 nm and length about 2.1 μm. The XRD patterns suggest that the N doping might suppress the anatase-rutile phase transition. A systematic research of the doping conditions was made through an orthogonal experiment. The experimental results indicate that the effect of reaction voltage is dominant, and the next factors are reaction time and electrolyte concentration, respectively. The optimal N-doping condition was then determined as follows: reaction voltage is 3 V, reaction time 2 h, and electrolyte concentration 0.5 M. Both the photoelectrochemical properties and photocatalytic activity under visible light irradiation were enhanced after N doping into TiO_2 nanotube arrays. XPS results indicate that the nitrogen element could be successfully doped into TiO_2 lattice, leading to visible light response. This, thus, supports the practicability of the electrochemical deposition method using for element doping into TNT arrays.

Acknowledgments

This work was supported by Program for New Century Excellent Talents in University (NCET-09-0110), National Nature Science Foundation of China (51162007), the Key Project of Chinese Ministry of Education (210171), and Hainan Natural Science Foundation (511110).

References

[1] A. Fujishima and K. Honda, "Electrochemical photolysis of water at a semiconductor electrode," *Nature*, vol. 238, no. 5358, pp. 37–38, 1972.

[2] K. Xu, S. Paul, and L. L. Cao, "Ordered TiO_2 nanotube arrays on transparent conductive oxide for dye-sensitized solar cells," *Chemistry of Materials*, vol. 22, no. 1, pp. 143–148, 2010.

[3] J. Wang and Z. Q. Lin, "Dye-sensitized TiO_2 nanotube solar cells with markedly enhanced performance via rational surface engineering," *Chemistry of Materials*, vol. 22, no. 2, pp. 579–584, 2010.

[4] Q. Zheng, B. X. Zhou, and J. Bai, "Self-organized TiO_2 nanotube array sensor for the determination of chemical oxygen demand," *Advanced Materials*, vol. 20, no. 5, pp. 1044–1049, 2008.

[5] S. Erdem, C. Zeliha, K. Necmettin, and Z. Z. Öztürk, "Synthesis of highly-ordered TiO_2 nanotubes for a hydrogen sensor," *International Journal of Hydrogen Energy*, vol. 35, no. 9, pp. 4420–4427, 2010.

[6] Z. H. Hu, K. Du, and Y. Cao, "Fabrication and photocatalytic application of highly ordered TiO_2 nanotube arrays," *Journal of Materials Science and Engineering*, vol. 4, no. 8, pp. 45–50, 2010.

[7] J. Bai, J. H. Li, and Y. B. Liu, "A new glass substrate photoelectrocatalytic electrode for efficient visible-light hydrogen production: CdS sensitized TiO_2 nanotube arrays," *Applied Catalysis B*, vol. 95, no. 3-4, pp. 408–413, 2010.

[8] J. W. Ng, X. W. Zhang, and T. Zhang, "Construction of self-organized free-standing TiO_2 nanotube arrays for effective disinfection of drinking water," *Journal of Chemical Technology and Biotechnology*, vol. 85, no. 8, pp. 1061–1066, 2010.

[9] X. W. Zhang, J. H. Du, and P. F. Li, "Grafted multifunctional titanium dioxide nanotube membrane: separation and photodegradation of aquatic pollutant," *Applied Catalysis B*, vol. 84, no. 1-2, pp. 262–267, 2008.

[10] Y. Y. Song, S. S. Felix, and B. Sebastian, "Amphiphilic TiO_2 nanotube arrays: an actively controllable drug delivery system," *Journal of the American Chemical Society*, vol. 131, no. 12, pp. 4230–4232, 2009.

[11] M. Kalbacova, J. M. Macak, and S. F. Schmidt, "TiO_2 nanotubes: photocatalyst for cancer cell killing," *Physica Status Solidi*, vol. 2, no. 4, pp. 194–196, 2008.

[12] R. Asahi, T. Ohwaki, and K. Aoki, "Visible-light photocatalysis in nitrogen-doped titanium oxides," *Science*, vol. 293, no. 5528, pp. 269–271, 2001.

[13] A. Ghicov, J. M. Macak, and H. Tsuchiya, "Ion implantation and annealing for an efficient N-doping of TiO_2 nanotubes," *Nano Letters*, vol. 6, no. 5, pp. 1080–1082, 2006.

[14] Y. Y. Chen, S. M. Zhang, and Y. Yu, "Synthesis, characterization, and photocatalytic activity of N-doped TiO_2 nanotubes," *Journal of Dispersion Science and Technology*, vol. 29, no. 2, pp. 245–249, 2008.

[15] Z. Jiang, F. Yang, and N. J. Luo, "Solvothermal synthesis of N-doped TiO_2 nanotubes for visible-light-responsive photocatalysis," *Chemical Communications*, vol. 11, no. 4, pp. 6372–6374, 2008.

[16] X. Feng, Y. Wang, and Z. S. Jin, "Photoactive centers responsible for visible-light photoactivity of N-doped TiO_2," *New Journal of Chemistry*, vol. 32, no. 6, pp. 1038–1047, 2008.

[17] Y. K. Lai, J. Y. Huang, H. F. Zhang et al., "Nitrogen-doped TiO_2 nanotube array films with enhanced photocatalytic activity under various light sources," *Journal of Hazardous Materials*, vol. 184, no. 1–3, pp. 855–863, 2010.

[18] J. Q. Geng, D. Yang, and J. H. Zhu, "Nitrogen-doped TiO_2 nanotubes with enhanced photocatalytic activity synthesized by a facile wet chemistry method," *Materials Research Bulletin*, vol. 44, no. 1, pp. 146–150, 2009.

[19] D. Kim, S. Fujimoto, and P. Schmuki, "Nitrogen doped anodic TiO_2 nanotubes grown from nitrogen-containing Ti alloys," *Electrochemistry Communications*, vol. 10, no. 6, pp. 910–913, 2008.

[20] S. P. Li, S. W. Lin, and J. J. Liao, "Effects of synthesis parameters on controllable growth of highly-ordered TiO_2 nanotube arrays," *Advanced Materials Research*, vol. 284–286, pp. 791–795, 2011.

[21] Y. K. Lai, L. Sun, and C. Chen, "Optical and electrical characterization of TiO_2 nanotube arrays on titanium substrate," *Applied Surface Science*, vol. 252, no. 4, pp. 1101–1106, 2005.

[22] J. J. Xu, Y. H. Ao, and M. D. Chen, "Photoelectrochemical property and photocatalytic activity of N-doped TiO_2 nanotube arrays," *Applied Surface Science*, vol. 256, no. 13, pp. 4397–4401, 2010.

[23] S. Sakthivel and H. Kisch, "Daylight photocatalysis by carbon-modified titanium dioxide," *Angewandte Chemie*, vol. 42, no. 40, pp. 4908–4911, 2003.

[24] Y. Y. Chen, S. M. Zhang, and Y. Yu, "Synthesis, characterization, and photocatalytic activity of N-doped TiO_2 nanotubes," *Journal of Dispersion Science and Technology*, vol. 29, no. 2, pp. 245–249, 2008.

[25] M. Sathish, B. Viswanathan, R. P. Viswanath, and C. S. Gopinath, "Synthesis, characterization, electronic structure, and photocatalytic activity of nitrogen-doped TiO_2 nanocatalyst," *Chemistry of Materials*, vol. 17, no. 25, pp. 6349–6353, 2005.

[26] J. W. Zhang, Y. Wang, and Z. S. Jin, "Visible-light photocatalytic behavior of two different N-doped TiO_2," *Applied Surface Science*, vol. 254, no. 15, pp. 4462–4466, 2008.

[27] J. L. Gole and J. D. Stout, "Highly efficient formation of visible light tunable $TiO_{2-x}N_x$ photocatalysts and their transformation at the nanoscale," *The Journal of Physical Chemistry B*, vol. 108, no. 4, pp. 1230–1240, 2004.